Applied Mathematics and Computational Intelligence
Volume 11, No. 1, Dec 2022 [133 – 145]

Theoretical Analysis of MHD Williamson Flow Across a Rotating Inclined Surface

Belindar A.Juma[1], Abayomi S.Oke[2*], Afolabi G.Ariwayo[3], Olum J.Ouru[4]

[1,4]Department of Mathematics and Actuarial Science, Kenyatta University, Kenya.
[2,3]Department of Mathematical Sciences, Adekunle Ajasin University, Akungba Akoko, Nigeria.

* Corresponding author: okeabayomisamuel@gmail.com, abayomi.oke@aaua.edu.ng

Received: 18 December 2021; Accepted: 15 March 2021; Available online (in press): 29 April 2022

ABSTRACT

The desire to enhance transfer of mass and heat across rotating plates during industrial processes has increased recently. This study considers the flow of Williamson fluid due to its ability to exhibit pseudo-plastic nature while admitting shear-thinning properties. This study theoretically examines the effect of rotation, and angle of plate inclination on MHD flow of Williamson fluid. The flow is modelled as a system of PDEs formulated by including Coriolis force and angle of inclination in the Navier-Stokes equation. The system is reduced using similarity transformation and the solution is obtained using MATLAB bvp4c that executes the three-stage Lobato IIIa finite difference method. The results are displayed as graphs and flow velocity shows a direct proportional relationship with the rotation but inversely proportional to Prandtl number, MF strength, inclination angle, and Williamson parameter. The local skin friction reduces at the rate -0.8052 as the rotation increases. Heat and mass transfer rates can be enhanced by increasing rotation and decreasing MF strength.

Keywords: Coriolis force, Inclination angle, Williamson fluid, MHD flow.

MSC Classification: 76A05; 76D05.

Nomenclature

T	Temperature	u, v	velocity components in the x, y-directions
Ω	angular velocity	β, β^*	coefficient of thermal and concentration expansion
B_0	MF strength	D_B, D_T	Brownian and thermophoretic diffusivity
κ	thermal conductivity	T_w, T_∞	Wall surface and free stream temperature
α	inclination angle	C_w, C_∞	Wall surface and free stream concentration
ρ	fluid density	g	Acceleration due to gravity
c_p	Specific heat capacity	C	Concentration of nanoparticle
K	Rotation parameter	σ	electrical conductivity
γ	Williamson fluid parameter	Pr	Prandtl number
M	MF parameter	N_b, N_t	Brownian and thermophoretic parameter
Sc	Schmidt number	Gr_t, Gr_s	Thermal and Solutal Grashof parameter

1 INTRODUCTION

When a fluid that has the tendency to conduct electricity moves in a magnetic field (MF) generates an electric current which in turn induces a magnetic field. The fluid experiences a magnetohydrodynamic (MHD) force, also referred to as Lorentz force [1]. The study of magnetohydrodynamic flow deserves to be thoroughly investigated because a substantial part of the cosmos is filled with charge particles. Applications of magnetohydrodynamics flow include astrophysics, jet printers, fusion reactors, and MHD pumps, MHD generators and MHD flow meters. Heat and mass transfer (HAMT) in an MHD flow has practical applications in thermal insulation engineering, biosensors, geothermal reservoirs and engineering, aerosol generation and dispersion, nuclear waste repository, distillation, and photovoltaic.

Katagiri [2] studied the MHD Couette motion formation in a viscous incompressible fluid and found out that the velocity declines with increasing MF strength. Malapati and Polarapu [3] presented an analysis of an unsteady MHD free convective HAMT in a boundary layer flow and found out that velocity profiles decrease with magnetic field, while concentration decreases with Schmidt number. Sheri and Modugula [4] analysed an unsteady MHD flow across an inclined plate and inferred that temperature profiles decrease with Prandtl number while velocity profiles increase with either the solutal Grashof number or thermal Grashof number. Sivaiah and Reddy [5] analysed HAMT of an unsteady MHD flow past a moving inclined porous plate. Flow velocity was found to rise with an increase in MF strength; as against the results from [2]. Their results showed that velocity profile increases with increasing solutal and thermal Grashof number; in agreement with the results from [2]. Also, velocity and concentration decrease with Schmidt number and temperature profile decreases with Prandtl number. Iva et al. [6] also supported the results of Katagiri [2] across a rotating plane. Sreedhar and Reddy [7] considered the impact of chemical reaction in the presence of heat absorption and found out that velocity profiles decrease with both Prandtl number and MF strength. Zafar et al. [8] analysed the effect of inclination angle on MHD flow. Hussain et al. [9] examined the magnetohydrodynamic flow of Maxwell nanofluid and deduced that flow velocity decreases as either MF strength and/or inclination angle increases. The results also show that flow velocity increases as Maxwell parameter increases while flow temperature is enhanced with rising inclination angle. In a study by Khan et al. [10], an extensive investigation is conducted to unravel the thermophysical properties of MHD Williamson flow past a simultaneously rotating and stretching surface. Results indicated that velocity is boosted as values of rotation gets larger and increment in Pr inhibits temperature distribution. Yusuf and Mabood [11] examined chemical reaction on MHD Williamson fluid flow over an inclined permeable wall. The results indicate that both the magnetic strength and the Williamson fluid parameter have adverse effect on the fluid velocity. Srinivasulu and Goud [12] explored the impact of Lorentz force on Williamson's nanofluid. With a rise in magnetic strength M, velocity profile diminishes but boosts the temperature and concentration profiles. The temperature and concentration profiles increase and velocity profile decreases with increase in inclination angle. Li et al. [13] considers the heat generation and/or heat absorptions on MHD Williamson nanofluid flow. More recent work on a rotating plane include [14–19].

Based on the available information, very little has not been done to figure out how Williamson fluid flows across an inclined plate. In this present study, a two-dimensional flow of Williamson flow past an inclined plate is considered. This study unravels the effects of strength of MF on the magnetohydrodynamic flow of Williamson fluid an inclined rotating plate.

2 GOVERNING EQUATIONS

This study considers a steady 2D laminar boundary layer flow of a viscous, thermally and electrically-conducting fluid across a rotating inclined plate. The arrangement of flow is shown in Figure (1) below. The flow configuration shows Williamson fluid flowing across a rotating plane inclined at an angle α while a MF of strength B_0 acts perpendicular to the flow. The plane is stretched linearly at $u = ax$, and the equations are formulated to allow the no-slip effect. The equations governing the magnetohydrodynamic fluid flow across the surface of an inclined plane is formulated hereby. The continuity equation

$$\frac{\partial u}{\partial x} + \frac{\partial v}{\partial y} = 0 \tag{1}$$

is obeyed by the flow, just as it is the case for every fluid flow.

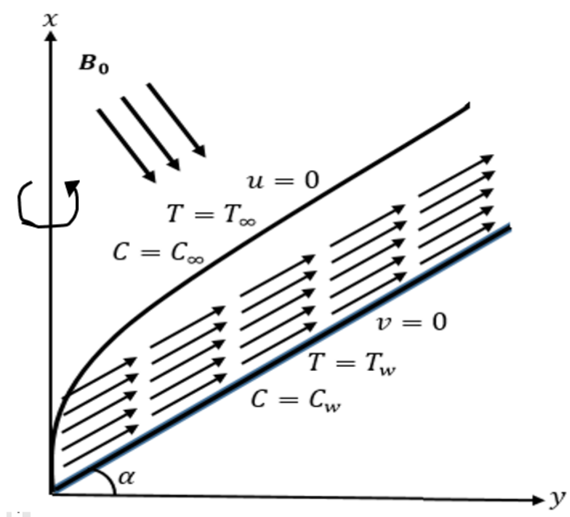

Figure 1 : Flow configuration

By incorporating the Boussinesq's approximation and the Lorentz force, the momentum equation [16] is

$$u\frac{\partial u}{\partial x} + v\frac{\partial u}{\partial y} - 2\Omega u = \nu\left(1 + \Gamma\sqrt{2}\frac{\partial u}{\partial y}\right)\frac{\partial^2 u}{\partial y^2} + g\beta\,(T - T_\infty)\cos\alpha$$
$$+ g\beta^*\,(C - C_\infty)\cos\alpha - \frac{\sigma B_0^2 u}{\rho} - \frac{\nu}{\rho}u. \tag{2}$$

The energy equation is obtained by using the Buongiorno modification as

$$u\frac{\partial T}{\partial x} + v\frac{\partial T}{\partial y} = \frac{\kappa}{\rho c_p}\frac{\partial^2 T}{\partial y^2} + \tau\left(\frac{D_B}{C}\frac{\partial C}{\partial y}\frac{\partial T}{\partial y} + \frac{D_T}{T_\infty}\left(\frac{\partial T}{\partial y}\right)^2\right). \tag{3}$$

The species equation also follows as

$$u\frac{\partial C}{\partial x} + v\frac{\partial C}{\partial y} = D_B\frac{\partial^2 C}{\partial y^2} + \frac{D_T\,C}{T_\infty}\frac{\partial^2 T}{\partial y^2}, \tag{4}$$

with the boundary conditions

$$\begin{cases} u = ax,\ v = 0,\ T = T_w,\ C = C_w,\ \text{at } y = 0, \\ u \to 0,\ T \to T_\infty,\ C \to C_\infty,\ \text{as } y \to \infty. \end{cases} \tag{5}$$

The quantities of industrial and engineering importance [4] are the coefficient of skin friction, Nusselt number and Sherwood number defined as

$$C_f = \frac{\nu}{a^2}\left(\frac{\partial u}{\partial y}\right)_{y=0},\ Nu = -\frac{x\left(\frac{\partial T}{\partial y}\right)_{y=0}}{(T_w - T_\infty)},\ Sh = -\frac{x\left(\frac{\partial C}{\partial y}\right)_{y=0}}{(C_w - C_\infty)}.$$

3 METHODOLOGY

The first step in solving the governing equations is to nondimensionalise using the similarity variables

$$u = axf',\ v = -(a\nu)^{\frac{1}{2}} f,\ \theta = \frac{T - T_\infty}{T_w - T_\infty},\quad = \frac{C - C_\infty}{C_w - C_\infty},\ \eta = y\left(\frac{a}{\nu}\right)^{\frac{1}{2}},$$

with the stream function ψ defined as

$$\psi = (a\nu)^{\frac{1}{2}} xf(\eta).$$

The governing equations nondimensionalise to the system

$$(1 + \gamma f'')f''' - f'f' + ff'' + Kf' + Gr_t\theta\cos\alpha + Gr_s \cos\alpha - Mf' - K_c f' = 0 \tag{6}$$

$$\theta'' + Prf\theta' + N_b\Phi'\theta' + N_t(\theta')^2 = 0 \tag{7}$$

$$'' + Sc\,'f + \frac{N_t}{N_b}\theta'' = 0. \tag{8}$$

and the boundary conditions become

$$f = 0;\ f' = 1;\ \theta = 1;\ = 1 \text{ at } \eta = 0 \tag{9}$$

$$f' \to 0;\ \theta \to 0;\ \to 0 \text{ as } \eta \to \infty, \tag{10}$$

where

$$Gr_t = \frac{g\beta(T_w - T_\infty)}{a^2x},\ Gr_s = \frac{g\beta^*(C_w - C_\infty)}{a^2x},\ K = \frac{2\Omega}{a}$$

$$M = \frac{\sigma B_0^2}{a\rho},\ K_c = \frac{\nu}{a\rho},\ Sc = \frac{\nu}{D_B},\ N_b = \frac{\tau D_B}{\alpha},\ Pr = \frac{\nu}{\alpha},$$

$$N_t = \frac{\tau D_T(T_w - T_\infty)}{\alpha T_\infty},\ \gamma = \Gamma\left(\frac{2a^3x^2}{\nu}\right)^{\frac{1}{2}},$$

The dimensionless form of the coefficient of shear stress C_f, the heat transfer rate Nu, the mass transfer rate Sh are

$$R_e^{\frac{1}{2}} C_f = 2\left(1 + \frac{\gamma}{2} f''(0)\right) f''(0),$$
$$R_e^{-\frac{1}{2}} Nu = -\theta'(0),\ Re^{-\frac{1}{2}} Sh = -\Phi(0).$$

To rewrite the dimensionless equations (6-8), we set

$$X_1 = f,\ X_2 = f',\ X_3 = f'',\ X_4 = \theta,$$
$$X_5 = \theta',\ X_6 = \ ,\ X_7 = \ ',$$

hence,

$$\begin{cases} X_1' = X_2, \\ X_2' = X_3, \\ X_3' = \frac{\left(X_2^2 - X_1X_3 - KX_2 - (Gr_tX_4 + Gr_sX_6)\cos\alpha + MX_2 + K_cX_2\right)}{1+\gamma X_3}, \\ X_4' = X_5, \\ X_5' = -PrX_1X_5 - N_bX_5X_7 - N_tX_5^2, \\ X_6' = X_7, \\ X_7' = -ScX_1X_7 - \frac{N_t}{N_b}X_6'. \end{cases} \tag{11}$$

with the conditions

$$\text{at } \eta = 0 : X_1(0) = 0,\ X_2(0) = 1,\ X_4(0) = 0, X_6(0) = 1 \tag{12}$$
$$\text{as } \eta \to \infty : X_2(\infty) \to 0,\ X_4 = 1,\ X_6(\infty) = 0. \tag{13}$$

Transform the boundary conditions (12-13) to the corresponding initial conditions by setting up the initial conditions as

$$X_1(0) = 0,\ X_2(0) = 1,\ X_3(0) = s_1,\ X_4(0) = 0,$$
$$X_5(0) = s_2,\ X_6(0) = 1,\ X_7(0) = s_3.$$

By making repeated arbitrary assumptions for s_1, s_2 and s_3, the problem is solved until the three remaining boundary conditions

$$X_2(\infty) \to 0,\ X_4 = 1,\ X_6(\infty) = 0.$$

are satisfied. The problem is solved numerically using the MATLAB bvp4c solver (for other methods of solution, see Oke [20]). For the sake of validation, set the parameters $Gr_t = Gr_s = K_c = K = 0$ and $\alpha = \pi/2$ and the model coincides with the model of Ahmed and Akbar [21]. The results obtained by using MATLAB bvp4c for the present model are compared with that obtained by Ahmed and Akbar [21] in Table (1) and the comparison shows that the present results are accurate enough.

Table 1 : Results Validation for $Re^{\frac{1}{2}} C_f$

γ	Ahmed and Akbar [21]	Present results
0	1.33930	1.33012694776585
0.1	1.29801	1.29879891166107
0.2	1.26310	1.26383734343962
0.3	1.22276	1.22345266814047

4 DISCUSSION OF RESULTS

The resulting system (11) is solved using the three-stage Lobatto IIIa finite difference accurate to the fourth order. The solution is presented in graphs that depict the influence of the flow parameters on flow dynamics. The flow parameter values chosen for default as

$$Gr_t = 1.0,\ Gr_s = 1.0,\ Sc = 0.62,\ M = 2,\ Pr = 4,\ \alpha = \pi/6,$$
$$K = 0.1,\ N_b = 0.1,\ N_t = 0.1,;K_c = 0.1, \gamma = 0.1.$$

The effects of rotation and Prandtl number on the velocity are shown in Figures (2) and (3). It is revealed velocity profiles increase with increasing rotation, meanwhile both the primary and secondary velocity profiles decrease with increasing Prandtl number. The increase in velocity profiles as rotation increases is because more kinetic energy is added to the flow as rotation amplifies. Surge in Prandtl number consequently reduces thermal diffusivity while momentum diffusivity increases; this is the reason for the decrease in the velocity profiles as Prandtl number increases. It can be seen that the rotation speed can be increased or decreased to adjust the flow velocities of fluid with high Prandtl number. The combined effects of the MF strength and inclination angle is shown in Figures (4 - 6). The Lorentz force generated with the presence of MF acts in the opposite direction to fluid flow and thereby causes a reduction in flow velocity (see Figures (4) and (5)). Increasing inclination angle reduces flow velocities in all direction since more work is done by the fluid to climb (see Figures (4) and (5)). The combined effect of MF strength and inclination angle is more reduction on flow velocity profiles in all direction. Meanwhile, heat energy is generated in the system as the Lorentz force opposes the motion (due to MF presence) and more heat energy is also generated as the fluid climbs the plate (due to an increase in inclination angle). Hence, the temperature profile increases as both MF strength and angle of inclination increase (as shown in Figure (6)).

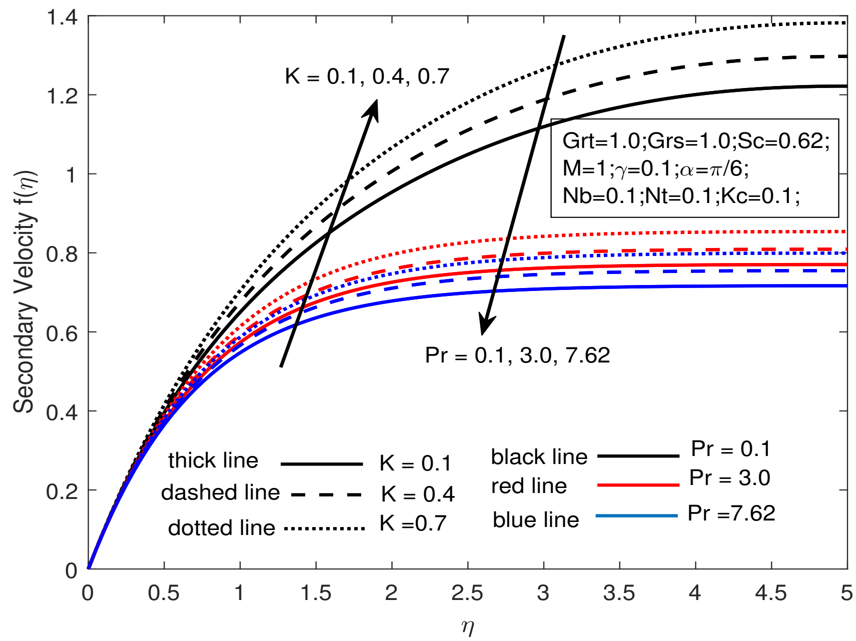

Figure 2 : Combined effects of rotation and Prandtl number on secondary velocity

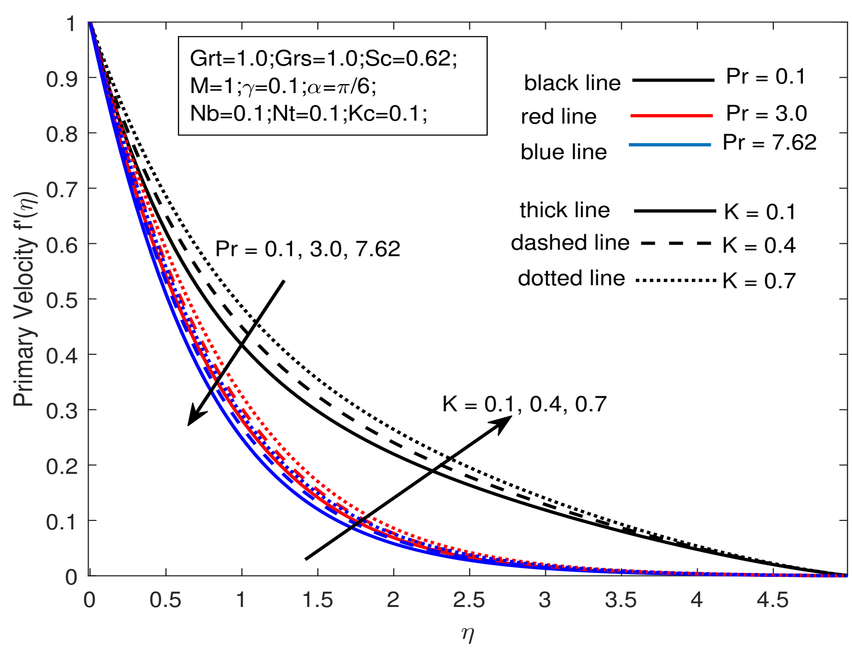

Figure 3 : Combined effects of rotation and Prandtl number on primary velocity

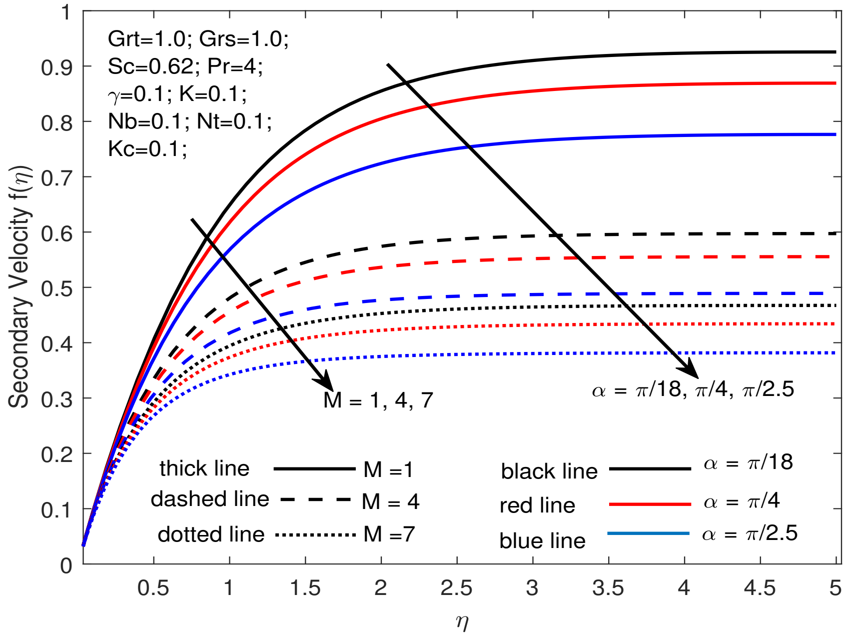

Figure 4 : Effects of MF strength and inclination angle on secondary velocity

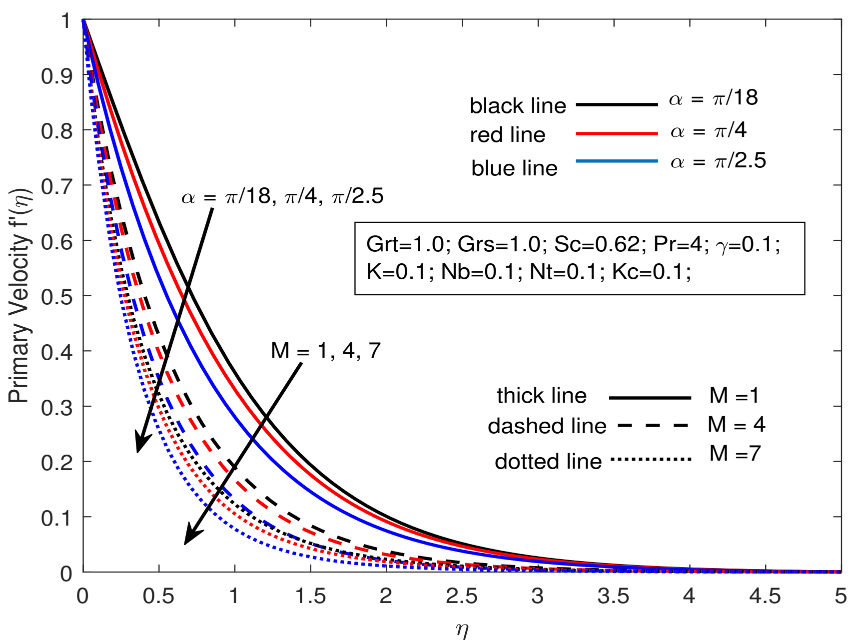

Figure 5 : Effects of MF strength and inclination angle on primary velocity

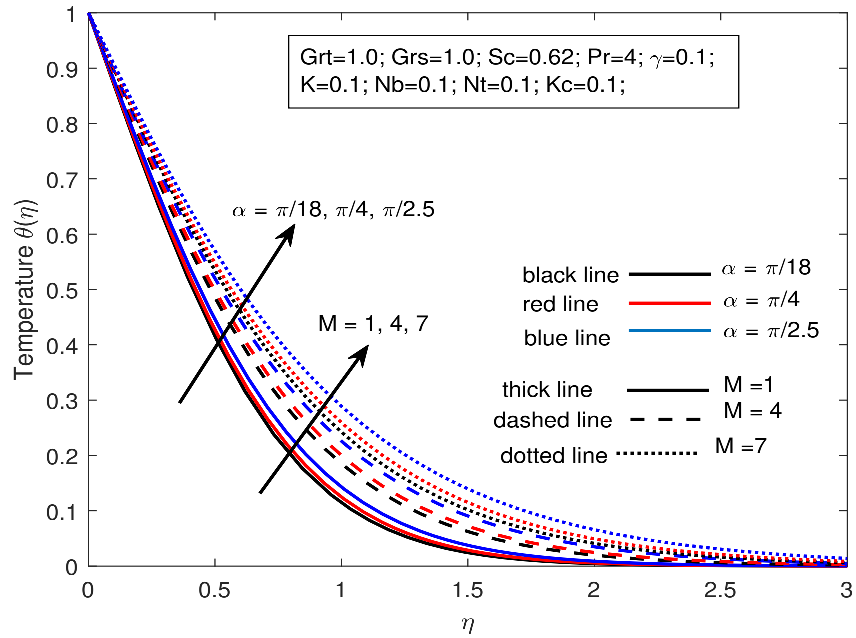

Figure 6 : Effects of MF strength and inclination angle on temperature

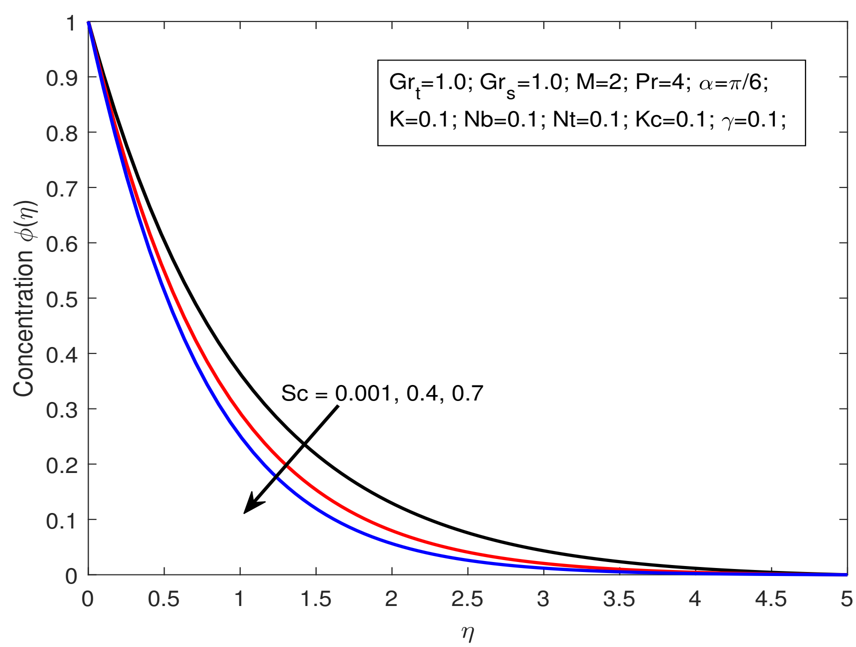

Figure 7 : Effect of Schmidt number on concentration

Tables (2) and (3) demonstrate how the rotation parameter and MF strength affect the quantities of interest. It is found that as rotation increases, the skin friction drag reduces at the rate of -0.8052, the Nusselt number at the rate 0.06 and Sherwood number increases at the rate 0.0218. Meanwhile, as MF strength increases, the skin friction drag increases at the rate of 0.7191, the Nusselt number decreases at the rate -0.0492 and Sherwood number decreases at the rate -0.016. With this, it is evident that the skin friction drag can be increased by increasing MF strength and decreasing rotation. In addition, the rate at which heat is transferred can be improved by increasing rotation and reducing MF strength. Finally, rate of convective mass transfer can be boosted by increasing rotation and reducing MF strength.

Table 2 : Quantities of interest with rotation parameter

K	skin friction	Nusselt number	Sherwood number
0	2.70422857	1.197017902	1.236991146
0.1	2.6264057	1.202717567	1.238985963
0.2	2.547751299	1.208510725	1.241036702
0.3	2.468223941	1.214401054	1.243146223
0.4	2.387779047	1.220392496	1.245317601
0.5	2.306368552	1.226489281	1.24755415
0.6	2.223940525	1.232695958	1.249859442
0.7	2.140438741	1.239017425	1.252237342
slope	-0.80520000	0.06000000	0.02180000

Table 3 : Quantities of interest with MF strength

M	skin friction	Nusselt number	Sherwood number
1	1.229763207	1.30996327	1.281131717
2	2.140438741	1.239017425	1.252237342
3	2.933080881	1.180446508	1.231316489
4	3.654850029	1.130115937	1.215141932
5	4.329552898	1.085844891	1.202086031
6	4.971093302	1.046309018	1.191223068
7	5.588451188	1.010620789	1.181978552
slope	0.71910000	-0.0492000	-0.01600000

5 CONCLUSION

The effects of rotation, MF strength, and inclination angle on MHD flow of Williamson fluid flow have been examined. The governing equations are formulated and solved numerically to generate graphs that describe the variation of flow properties as emerging flow parameters vary. The following are the outcome of the numerical examination;

1. The velocity profiles increase with increasing rotation.

2. The velocity profiles decrease with increasing Prandtl number.

3. Raising MF strength, inclination angle and Williamson parameter shrinks flow velocity profiles in all direction.

4. The temperature profile increases as both MF strength and angle of inclination increase.

5. The concentration decreases as Schmidt number increases.

6. Coefficient of skin friction increases with MF strength and decreasing rotation.

7. Heat transfer rate can be enhanced by increasing rotation and reducing MF strength.

8. Convective mass transfer can be enhanced by increasing rotation and decreasing MF strength.

In conclusion, it is clear that rotation reverses the effect of other flow parameters on the velocity profile. Hence, the effects of the other flow parameters can be alleviated by increasing the rotation of the plate.

Conflict of Interest Statement

All authors declare there is no conflict of interest.

REFERENCES

[1] H. Alfven, "Cosmic radiation as an intra-galactic phenomenon," *Ark. f. mat., astr. o. fys. 25B*, no. 29, 1937.

[2] M. Katagiri, "Flow formation in couette motion in magnetohydrodynamics," *Journal of the Physical Society of Japan*, vol. 17, no. 2, pp. 393–396, 1962.

[3] V. Malapati and P. Polarapu, "Unsteady MHD Free Convective Heat and Mass Transfer in a Boundary Layer Flow Past a Vertical Permeable Plate with Thermal Radiation and Chemical Reaction," *Procedia Engineering*, vol. 127, pp. 791–799, 2015.

[4] S. R. Sheri and P. Modugula, "Heat and mass transfer effects on unsteady mhd flow over an inclined porous plate embedded in porous medium with soret-dufour and chemical reaction," *International Journal of Applied and Computational Mathematics*, vol. 3, no. 2, pp. 1289–1306, 2017.

[5] G. Sivaiah and K. J. Reddy, "Unsteady MHD heat and mass transfer flow of a radiating fluid past an accelerated inclined porous plate with hall current," *International Journal of Research-Granthaalayah*, vol. 5, no. 7, pp. 42–59, 2017.

[6] L. M. Iva, M. S. Hasan, S. K. Paul, and R. N. Mondala, "Mhd free convection heat and mass transfer flow over a vertical porousplate in a rotating system with hall current, heat source and suction," *International Journal of Advances in Applied Mathematics and Mechanics*, vol. 6, no. 1, pp. 49–64, 2018.

[7] G. Sreedhar and B. R. B. Reddy, "Chemical reaction effect on unsteady MHD flow past an infinite vertical porous plate in the presence of heat absorption," *International Journal of Advanced Research in Engineering and Technology*, vol. 10, no. 1, pp. 95–103, 2019.

[8] A. A. Zafar, K. Shabbir, A. Naseem, and M. W. Ashraf, “Mhd natural convection boundary-layer flow over a semi-infinite heated plate with arbitrary inclination,” *Discrete & Continuous Dynamical Systems*, vol. 13, no. 3, pp. 1007–1015, Mar. 2020.

[9] S. M. Hussain, R. Sharma, M. R. Mishra, and S. S. Alrashidy, “Hydromagnetic dissipative and radiative graphene maxwell nanofluid flow past a stretched sheet-numerical and statistical analysis,” *Mathematics*, vol. 8, no. 11, 2020.

[10] M. Khan, T. Salahuddin, M. M. Y. andFarzana Khan, and A. Hussain, “Variable diffusion and conductivity change in 3d rotating williamson fluid flow along with magnetic field and activation energy,” *nternational Journal of Numerical Methods for Heat & Fluid Flow*, vol. 30, no. 5, pp. 2467–2484, 2020.

[11] T. A. Yusuf and F. Mabood, “Slip effects and entropy generation on inclined mhd flow of williamson fluid through a permeable wall with chemical reaction via dtm,” *Mathematical Modelling of Engineering Problems*, vol. 7, no. 1, pp. 1–9, 2020.

[12] T. Srinivasulu and B. S. Goud, “Effect of inclined magnetic field on flow, heat and mass transfer of williamson nanofluid over a stretching sheet,” *Case Studies in Thermal Engineering*, vol. 23, p. 100819, 2021.

[13] Y.-X. Li, M. H. Alshbool, M. Riaz Khan, I. Khan, Y.-P. Lv, and A. Issakhov, “Heat and mass transfer in mhd williamson nanofluid flow over an exponentially porous stretching surface,” *Case Studies in Thermal Engineering*, p. 100975, 2021.

[14] O. K. Koriko, K. S. Adegbie, A. S. Oke, and I. L. Animasaun, “Corrigendum: Exploration of coriolis force on motion of air over the upper horizontal surface of a paraboloid of revolution. (2020 phys. scr. 95 035210),” *Physica Scripta*, vol. 95, no. 8, p. 119501, Oct. 2020.

[15] A. S. Oke, W. N. Mutuku, M. Kimathi, and I. L. Animasaun, “Coriolis effects on mhd newtonian flow over a rotating non-uniform surface,” *Proceedings of the Institution of Mechanical Engineers, Part C: Journal of Mechanical Engineering Science*, p. 0954406220969730, 2020.

[16] J. O. Ouru, W. N. Mutuku, and A. S. Oke, “Buoyancy-induced MHD stagnation point flow of williamson fluid with thermal radiation,” *Journal of Engineering Research and Reports*, pp. 9–18, mar 2020.

[17] A. S. Oke, I. L. Animasaun, W. N. Mutuku, M. Kimathi, N. A. Shah, and S. Saleem, “Significance of coriolis force, volume fraction, and heat source/sink on the dynamics of water conveying 47 nm alumina nanoparticles over a uniform surface,” *Chinese Journal of Physics*, 2021.

[18] O. K. Koriko, K. S. Adegbie, A. S. Oke, and I. L. Animasaun, “Exploration of Coriolis force on motion of air over the upper horizontal surface of a paraboloid of revolution,” *Physica Scripta*, vol. 95, p. 035210, 2020.

[19] A. S. Oke, W. N. Mutuku, M. Kimathi, and I. L. Animasaun, “Insight into the dynamics of non-Newtonian Casson fluid over a rotating non-uniform surface subject to Coriolis force,” *Nonlinear Engineering*, vol. 9, no. 1, pp. 398–411, oct 2020.

[20] A. S. Oke, “Convergence of differential transform method for ordinary differential equations,” *Journal of Advances in Mathematics and Computer Science*, vol. 24, no. 6, pp. 1–17, 2017.

[21] K. Ahmed and T. Akbar, “Numerical investigation of magnetohydrodynamics Williamson nanofluid flow over an exponentially stretching surface,” *Advances in Mechanical Engineering*, vol. 13, no. 5, p. 168781402110198, may 2021.